

AD-A258 329



RL-TR-92-141
Final Technical Report
June 1992



2

NONLINEAR JOINT TRANSFORM CORRELATOR

University of Connecticut

Bahram Javidi

DTIC
ELECTE
DEC 8 1992
S C D

APPROVED FOR PUBLIC RELEASE; DISTRIBUTION UNLIMITED.



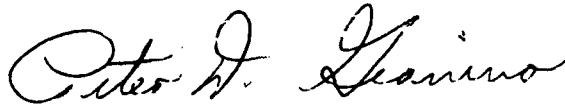
92-30965

30965

Rome Laboratory
Air Force Systems Command
Griffiss Air Force Base, NY 13441-5700

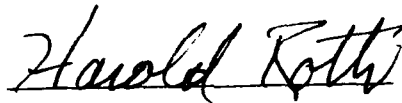
RL-TR-92-141 has been reviewed and is approved for publication.

APPROVED:



PETER D. GIANINO
Project Engineer

FOR THE COMMANDER



HAROLD ROTH, Director
Solid State Sciences
Electromagnetics and Reliability Directorate

DESTRUCTION NOTICE - For classified documents, follow the procedures in DOD 5200.22-M, Industrial Security Manual, or DOD 5200.1-R, Information Security Program Regulation. For unclassified, limited documents, destroy by any method that will prevent disclosure of contents or reconstruction of the document.

If your address has changed or if you wish to be removed from the RL mailing list, or if the addressee is no longer employed by your organization, please notify RL(EROP), Hanscom AFB MA 01731-5000. This will assist us in maintaining a current mailing list.

Do not return copies of this report unless contractual obligations or notices on a specific document require that it be returned.

REPORT DOCUMENTATION PAGE

Form Approved
OMB No. 0704-0188

Public reporting burden for this collection of information is estimated to average 1 hour per response, including the time for reviewing instructions, searching existing data sources, gathering and maintaining the data needed, and completing and reviewing the collection of information. Send comments regarding this burden estimate or any other aspect of this collection of information, including suggestions for reducing this burden, to Washington Headquarters Services, Directorate for Information Operations and Reports, 1215 Jefferson Davis Highway, Suite 1204, Arlington, VA 22202-4302, and to the Office of Management and Budget, Paperwork Reduction Project (0704-0188), Washington, DC 20503.

1. AGENCY USE ONLY (Leave Blank)		2. REPORT DATE June 1992		3. REPORT TYPE AND DATES COVERED Final Jun 89 - Apr 92	
4. TITLE AND SUBTITLE NONLINEAR JOINT TRANSFORM CORRELATOR				5. FUNDING NUMBERS C - F19628-89-K-0035 PE - 61102P PR - IL16 TA - 11 WU - 20	
6. AUTHOR(S) Bahram Javidi					
7. PERFORMING ORGANIZATION NAME(S) AND ADDRESS(ES) University of Connecticut Department of Electrical Engineering 345 Mansfield Rd Storrs CT 06269-2151				8. PERFORMING ORGANIZATION REPORT NUMBER N/A	
9. SPONSORING/MONITORING AGENCY NAME(S) AND ADDRESS(ES) Rome Laboratory (EROP) Hanscom AFB MA 01731-5000				10. SPONSORING/MONITORING AGENCY REPORT NUMBER RL-TR-92-141	
11. SUPPLEMENTARY NOTES Rome Laboratory Project Engineer: Peter D. Gianino/EROP/(617) 377-5119					
12a. DISTRIBUTION/AVAILABILITY STATEMENT Approved for public release; distribution unlimited.				12b. DISTRIBUTION CODE	
13. ABSTRACT (Maximum 200 words) Experiments are provided to investigate the nonlinear joint transform correlator (JTC). Experiments are used to determine the correlation peak intensity, signal to noise ratio (SNR), peak to sidelobe ratio (PSR), and correlation width for various degrees of the nonlinearity used at the Fourier plane. The system is implemented using an optically addressed spatial light modulator in the Fourier plane. The experiments show that for the images used here, nonlinear compression of the joint power spectrum is necessary to pull the signal out of scene noise and produce a peak to sidelobe ratio of larger than unity. In addition the sensitivity of the nonlinear JTC to the scaling and rotational changes of the input objects for various degrees of the nonlinearity applied to the joint power spectrum is investigated. The effect of the modulation transfer function of the spatial light modulator on the nonlinear JTC performance in the presence of multiple input targets is discussed.					
14. SUBJECT TERMS Joint Transform Correlator, Optical Correlator, Optical Signal Processing, Spatial Light Modulation				15. NUMBER OF PAGES 48	
				16. PRICE CODE	
17. SECURITY CLASSIFICATION OF REPORT UNCLASSIFIED	18. SECURITY CLASSIFICATION OF THIS PAGE UNCLASSIFIED	19. SECURITY CLASSIFICATION OF ABSTRACT UNCLASSIFIED	20. LIMITATION OF ABSTRACT UL		

Table of Contents

	Page No.
I. Introduction	1
II. Review	2
III. Experiments	3
IV. Summary	11
V. References	13
VI. Patents	12
VII. Involvement in Conferences, workshops, and Journals	13
VIII. Refereed Journal Papers	14
IX. Invited Papers in Conferences	16
X. Honors	16
XI. Milestones	16

DTC 400000-1-1000000

Accession For	
NTIS GRAB	<input checked="" type="checkbox"/>
DTIC TAB	<input type="checkbox"/>
Unannounced	<input type="checkbox"/>
Justification	
By	
Distribution/	
Availability Codes	
Dist	Avail and/or Special
A-1	

I. Introduction

Theoretical and experimental studies show that the nonlinear joint transform correlator (JTC) produces good correlation performance. Nonlinear correlators produce good correlation performance in the areas of peak intensity, peak to sidelobe ratio, correlation width, and discrimination against similar targets.¹⁻⁹ In nonlinear joint transform correlators (JTC), the nonlinearity is used at the Fourier plane of the JTC¹⁰ to nonlinearly transform the joint power spectrum.

In this report, we provide an experimental investigation of the effects of nonlinear transformation of the joint power spectrum on the performance of the JTC. Experiments are used to determine the correlation peak intensity, signal to noise ratio (SNR), peak to sidelobe ratio (PSR), and correlation width for various degrees of the nonlinearity used at the Fourier plane. The experiments are performed both in the absence and the presence of the input scene noise. The experiments show that for the images used here, nonlinear compression of the joint power spectrum is necessary to pull the signal out of scene noise and produce a peak to sidelobe ratio of larger than unity.

In addition, we provide an experimental investigation of the nonlinear JTC sensitivity to the scaling and rotation changes of the input objects for various degrees of nonlinearity applied to the joint power spectrum. The spatial light modulator (SLM) used at the Fourier plane is a Hughes liquid crystal light valve¹¹ (LCLV) operating in different degrees of nonlinear mode. The LCLV is operated in different degrees of nonlinear mode by adjusting its bias supply frequency. The experiments indicate that, as the severity of the nonlinear transformation of the joint power spectrum increases, the sensitivity of the nonlinear JTC to the scaling and rotation changes of the input objects increases. However, the nonlinear JTC may produce a better peak to sidelobe ratio in the presence of input signal rotation/scale changes. These experiments are important in the design of distortion invariant pattern

recognition systems.

The effects of the modulation transfer function (MTF) of the SLM on the nonlinear JTC performance are discussed. It will be shown that the MTF of the SLM limits the separation of the objects in the input plane. It also affects the correlation signals produced by the multiple targets input images.

II. Review

The implementation of the nonlinear JTC using an optically addressed SLM in the Fourier plane is shown in Fig. (1). Plane P_1 is the input plane that contains the reference signal $r(x+x_0,y)$ and the input signal $s(x-x_0,y)$. The Fourier transform interference is displayed at the input of the liquid crystal light valve (LCLV) to obtain the intensity of the Fourier transform interference. The joint power spectrum of the reference signal and input signal function is:

$$E(\alpha,\beta)=S^2(\alpha,\beta)+R^2(\alpha,\beta)+2S(\alpha,\beta)R(\alpha,\beta)\cos[2x_0\alpha+\Phi_S(\alpha,\beta)-\Phi_R(\alpha,\beta)] \quad (1)$$

where (α,β) are the spatial frequency coordinates, and $S(\alpha,\beta)e^{i\Phi_S(\alpha,\beta)}$ and $R(\alpha,\beta)e^{i\Phi_R(\alpha,\beta)}$ correspond to the Fourier transforms of the input signal $s(x,y)$ and reference signal $r(x,y)$, respectively. The LCLV applies a nonlinear transformation to the joint power spectrum according to the nonlinear characteristics of the device. The nonlinear characteristics of the device is denoted by $g(E)$ where E is the joint power spectrum. The LCLV output can be considered as the output of a nonlinear system:¹

$$g(E)=\sum_{v=0}^{\infty} H_v[R(\alpha,\beta),S(\alpha,\beta)]\cos[2vx_0\alpha+v\Phi_S(\alpha,\beta)-v\Phi_R(\alpha,\beta)] \quad (2)$$

where

$$H_v[R(\alpha, \beta), S(\alpha, \beta)] = \frac{\epsilon_v}{2\pi} (i)^v \int G(\omega) \exp\{i\omega[R^2(\alpha, \beta) + S^2(\alpha, \beta)]\} J_v[2\omega R(\alpha, \beta)S(\alpha, \beta)] d\omega \quad (3)$$

Here $G(\omega)$ is the Fourier transform of the nonlinearity. In this paper, we will consider the rotation and scale sensitivity of the first order correlation signal for $v=1$. Varying the severity of the nonlinearity will produce correlation signals with different characteristics.¹ In the experiments, the optically addressed SLM operating in a nonlinear mode may be used to nonlinearly transform the joint power spectrum. For highly nonlinear transformations, the high spatial frequencies are emphasized and the correlation becomes more sensitive in discrimination to similar targets.

III. Experiments

In Fig. 1, an argon ion laser ($\lambda=514$ nm) is expanded and collimated. It is passed through a photographic transparency (Kodak Black-and-white Negative Film 5060) containing the reference image and the input image. The images used in the correlation tests are shown in Fig. 2. The tank without background is the reference image. The sizes of the reference image and the input image are $2\text{mm} \times 3\text{mm}$ and $3\text{mm} \times 5\text{mm}$, respectively. The separation of the input image and the reference image is 3mm . A Fourier transform lens (FTL₁) with focal length of $f_1=1000\text{mm}$ is placed behind the transparency. The use of a lens with long focal length is due to the consideration of the limited resolution of the LCLV used in the experiments. A He-Ne laser beam ($\lambda=633$ nm) is expanded, collimated, and used as the read-out beam of the LCLV. The intensity of the read-out beam is approximately $25\mu\text{W}/\text{cm}^2$ over the aperture size ($25\text{mm} \times 25\text{mm}$) of the LCLV. A second Fourier transform

lens (FTL₂) with focal length $f_2=400\text{mm}$ is placed behind the beam splitter.

The input-output characteristic of the LCLV was tested for three bias supply frequencies applied to the LCLV as shown in Fig. 3. In Fig. 3, the readout amplitude values of the LCLV were measured for varying writing light intensities when the LCLV was operated in 10 Vrms power supply and three different supply frequencies applied to the LCLV¹². The tests were performed for the central part of the device with an area of 2 mm^2 . There were small variations for different parts of the SLM because of the non-uniformity of the device. The readout amplitude values of the LCLV were normalized to $5\text{ }\mu\text{W}/\text{cm}^2$. It can be seen from Fig. 3 that lowering the frequency of the bias voltage increases the nonlinearity of the input-output characteristics of the LCLV. When the LCLV is used in the Fourier plane of the JTC, these curves represent an approximation of the nonlinear transformation of the joint power spectrum.

In the experiments, we tested the correlation peak intensity and the correlation peak to sidelobe ratio of the JTC in the presence of the scaling and rotation of the input signal. The reference signal was fixed. The tests were performed for two cases: 1) correlation of the tank and the tank, and 2) correlation of the tank and the tank in the input scene noise[see Fig. 2]. The 3-D plots are normalized to a maximum value of unity. The DC terms are not shown in the 3-D correlation plots. The 3-D correlation plots were captured from optical experimental results using a CCD camera and a frame grabber interfaced with a computer. The correlation area covered by the plots is 64×64 pixels and the output plane is 512×512 pixels.

Figs. 4(a) and 5(a) illustrate the values of the normalized correlation peak intensity and the correlation peak to sidelobe ratio (PSR) versus scaling of the input signal for the correlation of the tank and the tank, respectively. The PSR is defined as the ratio of the correlation peak intensity to the noise intensity average values around the correlation peak:

$$PSR = \frac{[I(x_i, y_j)]_{\max}}{\sum_i^{N_1} \sum_j^{N_2} n(x_i, y_j) / N'_1 N'_2} \quad (4)$$

where $I(x_i, y_j)$ is the correlation peak intensity, $n(x_i, y_j)$ is the noise intensity outside the 50% response portion of the correlation peak intensity, N_1 and N_2 are the total number of pixels of the area where correlation peak is measured, and N'_1 and N'_2 are the number of pixels under the 50% response portion of the correlation spot. Here, we use $N_1 = N_2 = 64$ pixels.

Figs. 4(b) and 5(b) illustrate the values of the normalized correlation peak intensity and the correlation PSR versus scaling of the input signal for the correlation of the tank and the tank in the input scene noise, respectively. It can be seen from these figures that, as the severity of the nonlinear transformation increases, the correlation sensitivity increases to the scaling changes of the input signal. For operation along the same nonlinear curve, the joint transform correlation of the tank and the tank in input scene noise is more sensitive to the scaling changes than the joint transform correlation of the tank and the tank without noise. As the scaling factor increases, the correlation peak intensity and the PSR decrease. However, the PSR for the nonlinear cases remain larger than unity for a scaling change of up to 20%.

Figures 6 illustrates the nonlinear JTC output of the tank and the tank in the input scene noise for no rotational or scale changes of the input image. In Fig. 6(a), the liquid crystal light valve is operating along the 200Hz curve. In Fig. 6(b), the liquid crystal light valve is operating along the 60Hz curve. The 3-D plots of the correlation signals are also shown. For comparison, Fig. 7 illustrates the nonlinear JTC output of the tank and the tank in the input scene noise for a scale change of 1.05 of the input image. In Fig. 7(a), the liquid crystal light valve is operating along the 200Hz curve. In Fig. 7(b), the liquid crystal light valve is operating along the 60Hz curve.

The effects of the rotation of the input signal on the correlation peak intensity and the correlation PSR for the correlation of the tank and the tank is shown in Figs. 8(a) and 9(a), respectively. Figs. 8(b) and 9(b) illustrate the effects of the rotation of the input signal on the correlation peak intensity and the correlation PSR for the correlation of the tank and the tank in the input scene noise, respectively. It can be seen that, as the severity of the nonlinear transformation increases, the correlation sensitivity increases to the rotational changes of the input signal. For operation along the same nonlinear curve, the correlation of the tank and the tank in the input scene noise is more rotationally sensitive than the correlation of the tank and the tank. The PSRs for both nonlinear cases remain larger than unity for up to four degrees of rotation.

Figure (10) illustrates the photographs and the 3-D plots of the nonlinear JTC output of the tank and the tank in the input scene noise for a rotational change of 2 degrees. In Fig. 10(a), the liquid crystal light valve is operating along the 200Hz curve. In Fig. 10(b), the liquid crystal light valve is operating along the 60Hz curve.

Experiments are performed to investigate the effects of the spatial frequency response of the Fourier plane SLM on the correlation signals. The modulation transfer function¹³ (MTF) is used to represent the spatial frequency response of the device. To measure the MTF, a Ronchi grating was generated by the computer and was displayed on the monitor. Then the grating function was imaged onto the input of the LCLV. The grating function was read out and the first order diffraction was recorded at the Fourier plane. The measurements were repeated for different spatial frequencies of the Ronchi grating. The normalized intensity of the first order diffraction as a function of the grating spatial frequency is shown in Fig. 11. The intensity is normalized by the maximum intensity at the DC spatial frequency multiplied by 100. This curve represents the MTF of the LCLV used in our experiments. For joint power spectrum spatial frequencies larger than 15 lp/mm, the device response decreases

rapidly. A modulation of 50% is obtained at 18 lp/mm and a modulation of 80% is obtained at 13 lp/mm. We may limit the maximum spatial frequency of the input joint power spectrum to the frequency where the normalized MTF of the LCLV drops down to 80%. This may reduce the effect of the MTF on the correlation performance. The cut-off frequency of the SLM is defined as the frequency where the normalized MTF value drops down to less than 5%. For the LCLV used in our experiments, the cutoff frequency is over 30 lp/mm.

The joint power spectrum is expressed by Eq. (1). We assume that the Fourier magnitudes and the Fourier phases of the input signal and the reference signal are slowly varying compared with $\cos(2x_0\alpha)$. Under these conditions, the frequency of the interference intensity is approximated by $\frac{2x_0}{\lambda f}$, where λ is the write-in light wavelength and f is the focal length of the Fourier transform lens. This frequency must be less than the cutoff frequency of the LCLV (μ_m) to produce a correlation response; i.e., $\frac{2x_0}{\lambda f} < \mu_m$. For the images used in the experiments, $2x_0 < 15.4$ mm.

The separation of the reference object and the input target closest to the optical axis must be large enough to avoid the overlap of the correlation peaks and the DC terms. Given a reference object $r(x+x_0, y)$ and a single input signal $s(x-x_0, y)$, the separation condition for a linear JTC requires that:

$$2x_0 \geq \frac{1}{2}(L_r + 3L_s) \quad (5)$$

where L_r and L_s are the widths of the reference signal and the input signal, respectively. In the experiments, we used $L_r = 2$ mm and $L_s = 3$ mm. For the linear JTC, a separation of $2x_0 \geq 5.5$ mm is obtained for a single input signal. The correlation width of the nonlinear JTC (for severe compression) is much narrower than that produced by the linear JTC. Thus, for a single input signal, the separation of the input images can be made smaller than the

requirement in Eq.(5). In the experiments, we used $2x_0=3\text{mm}$. The LCLV used in our experiments produced a somewhat large DC on the optical axis at the output plane. The on axis DC term had to be considered in choosing x_0 .

As the separation of the input image and the reference image increases, the spatial carrier frequency of the joint power spectrum increases. The MTF value is reduced as the spatial carrier frequencies is increased, which degrades the correlation response and reduces the correlation amplitude.

Suppose that the MTF amplitude of the LCLV is $M(\alpha,\beta)$. The effective joint power spectrum using Eq. (1) is:¹³

$$E(\alpha,\beta)=S^2(\alpha,\beta)+R^2(\alpha,\beta)+2S(\alpha,\beta)R(\alpha,\beta)M\left(\frac{2x_0}{\lambda f},0\right)\cos[2x_0\alpha+\Phi_S(\alpha,\beta)-\Phi_R(\alpha,\beta)],$$

(6)

where it is assumed that the amplitudes and the phases of the signals Fourier transforms vary slowly compared with $2x_0$ and only the MTF amplitude is considered.

We tested the effect of the separation of the input signal and the reference signal for the image shown in Fig. (2). The correlation peak intensity was measured when the LCLV was operated along the 60Hz curve. Figure. (12) illustrates the normalized correlation peak intensity of the tank and the tank in the input scene noise, versus the separation of the reference image and the input image. It can be seen from this figure that, as the input signals separation increases, the correlation peak intensity decreases. Due to the non-uniform illumination of a Gaussian beam profile at the input plane, the correlation peak intensity will decrease as the separation of the reference and input object increases⁶. The experimental results presented in Fig. 12 take into account both the Gaussian profile of the illumination and the MTF of the LCLV. When the signals separation is larger than 6mm, the correlation peak intensity decreases rapidly. The signals separation of 6mm corresponds to a spatial

frequency of 12 lp/mm which places the joint power spectrum at the 80% response portion of the MTF.

When multiple targets are present in the input scene, the targets are located in different positions. Each target generates a different spatial carrier frequency in the joint power spectrum. The carrier frequency due to each target depends on the position of the target in the input scene and the location of the reference image. The frequency response magnitude of the device (MTF) will vary for different spatial carrier frequencies representing different targets. For the targets that are farther away from the reference image, a larger carrier frequency is generated and the MTF magnitude becomes smaller. The effect is a reduction in the correlation peak intensity as the input target separation from the optical axis increases.

We assume that multiple targets $[s_1(x-x_1, y-y_1), s_2(x-x_2, y-y_2), \dots, s_n(x-x_n, y-y_n)]$ are present in the input scene and that the reference image is $r(x-x_0, y-y_0)$. In this case, the output signal contains the following terms:²

1) The autocorrelations of the reference image $[R_{rr}(x, y)]$ and the autocorrelations of the input targets $[R_{s_i s_i}(x, y), i=1, 2, \dots, n]$; 2) The cross-correlations between the reference image and the input targets $[R_{rs_i}(x, y), i=1, 2, \dots, n]$; and 3) The cross-correlations between the different targets $[R_{s_i s_j}(x, y), ij, i=1, 2, \dots, n, j=1, 2, \dots, n]$.

The autocorrelation terms in (1) are diffracted on the optical axis at the output plane. The correlation functions between the reference image and the input targets $[R_{rs_i}]$ and the correlation functions between the different targets $[R_{s_i s_j}]$ may overlap unless the input scene targets are placed sufficiently far from the reference image. The required separation between the input images and the reference image can be expressed as:

$$\max (D_{s_i s_j}) < \min (D_{s_i r}) \quad (i, j=1, 2, \dots, n) \quad (7)$$

where $D_{s_i s_j}$ is the distance between any two of the targets s_i and s_j , and $D_{s_i r}$ is the distance

between the reference image and any one of the targets s_i in the input scene. Here, it is assumed that the width of the nonlinear correlation signals are narrow compared with the input signals separations.

We have performed correlation experiments for multiple targets in the input scene to test the effect of the LCLV spatial frequency response (MTF) on the correlation peak intensity. The reference object was the tank image and the input targets were three tanks as shown in Fig. (13). The reference object is denoted by r , and the input targets are denoted by s_1 , s_2 , and s_3 . The spacing of the multiple targets in Fig. 13 is as follows: the distance between s_1 and s_2 is d , the distance between s_2 and s_3 is $2d$, and the distance between r and s_1 is $4d$. Here, $d=1.5$ mm. Nonlinear JTC experiments were performed by using the saturation property of the input-output characteristics of the LCLV to threshold the joint power spectrum. In the multiple targets JTC experiments, the power supply voltage of the LCLV was 10 Vrms and the supply frequency was 60 Hz. The input-output characteristics of the LCLV for 60 Hz is shown in Fig. (3). The input light illumination to the LCLV was adjusted by a neutral density filter to place the joint power spectrum distribution in the saturation region of the LCLV input-output characteristic.³ The joint power spectrum is nonlinearly transformed to produce the nonlinear correlation signals.

Figure (14) presents the photograph of the nonlinear JTC output and the corresponding 3-D mesh plot of the output. The outer three correlation peaks (denoted by rs_1 , rs_2 and rs_3) correspond to the correlations between the reference tank (r) and the input tanks (s_1 , s_2 and s_3). The other three correlation peaks near the optical axis (s_1s_2 , s_1s_3 , and s_2s_3) correspond to the correlations between the targets in the input scene.

It is evident from Fig. (14) that the correlation intensities of the targets decrease as their separations from the optical axis increase. Since the frequency response of the device and the Gaussian profile of the illumination are known, the peak intensity decrease may be

compensated by post processing in the correlation plane. The MTF effect of the device and the non-uniform effect of the illumination may be compensated as long as the correlation peak to sidelobe ratio is larger than unity.

IV. Summary

we have provided an experimental investigation of the JTC sensitivity to the scaling and rotation changes of the input objects for various degrees of nonlinearity applied to the joint power spectrum. Experiments are used to determine the correlation peak intensity for various degrees of the nonlinearity used at the Fourier plane. The experimental results indicate that, as the severity of the nonlinear transformation of the joint power spectrum increases, the sensitivity of the nonlinear JTC to the scaling and rotation changes of the input objects increases. Both the correlation peak intensity and the correlation peak to sidelobe ratio are determined by experiments.

The effect of the limited spatial frequency response of the Fourier plane SLM on the separation of the input targets from the optical axis is investigated. Experiments are provided to show that the modulation transfer function of the SLM results in a reduction in the correlation peak intensity as the separation between the input image and the reference image increases. Nonlinear JTC experiment using a multiple targets input image is used to illustrate the decrease in the correlation peak intensity of the targets that are farther away from the optical axis.

V. References

1. B. Javidi, "Nonlinear joint power spectrum based optical correlation," *Applied Optics*, Vol. 28, No. 12, pp. 2358-2367, 15 June 1989.
2. B. Javidi, J. Wang, and Q. Tang, " Multiple Objects Binary Joint Transform Correlation

- Using Multiple Level Threshold Crossings", Applied Optics, Vol. 31, pp. 4234-4244, October 10, 1991.
3. B. Javidi, Q. Tang, D. A. Gregory and T. Hudson, "Experiments on nonlinear joint transform correlators using an optically addressed SLM in the Fourier plane, " Applied Optics, Vol. 30, No. 14, pp. 1772-1776, 10 May 1991.
 4. B. Javidi, " Comparison between the nonlinear joint transform correlator and the nonlinear matched filter based correlator", Optical Engineering, Vol. 29, No. 9, pp. 1013-1020, September 1990.
 5. B. Javidi and J. L. Horner, "Single SLM joint transform correlator," Applied Optics, Vol. 28, No. 5, pp.1027-1032, 1 March 1989.
 6. K. H. Fielding and J. L. Horner, "1-f binary joint correlator," Optical Engineering, Vol. 29, No. 9 pp.1081-1087, September 1990.
 7. W. B. Hahn and D. L. Flannery, "Basic Design Elements of the Binary Joint Transform Correlator", Proc. SPIE, Vol. 1347, Optical Information-Processing Systems and Architectures, pp. 344-356, July 1990.
 8. A. Vander Lugt and F. B. Rotz, " The use of film nonlinearities in optical spatial filtering", Applied Optics, Vol. 9, No. 1, pp. 215-222, January 1970.
 9. A. Kozma, "Photographic recording of spatially modulated coherent light", J. Opt. Soc. Am., Vol. 56, pp. 428-432 (1966)
 10. C. S. Weaver and J. W. Goodman, " A technique for optically convolving two functions", Applied Optics, Vol. 5, No.7, pp. 1248-1249, (1966).
 11. W. P. Bleha et. al., "Application of the liquid crystal light valve to real time optical data processing," Optical Engineering, Vol. 17, No. 4. pp. 371-384 (1978)
 12. T. D. Hudson and D. A. Gregory, "Nonlinear response of liquid crystal spatial light modulators," Proc. SPIE, Vol. 1347, Optical Information-Processing Systems and Architectures, July 1990.

13. J. W. Goodman, Introduction to Fourier Optics, McGraw-Hill, NY (1966).

VI. Patents:

B. Javidi and J. L. Horner, "Generalization of the Linear Matched Filter Concept to Nonlinear Matched Filters," pending

B. Javidi and J. L. Horner, "Image Deconvolution with a Log/Exponential Nonlinear Joint Transform Correlator", pending

VII. Involvement in Conferences, workshops, and Journals

Conference Chairman, " Optical Information Processing Systems I and II," International Symposium on Optical and Optoelectronic Applied Science and Engineering, San Diego, California, August 1989 and July 1990

Conference Co-Chairman, "Critical Review of Technology on Optical Pattern Recognition", OPTCON 1991, San Jose, California November 1991

Session Chairman, Session on Nonlinear Optical Processing, Institute of Electrical and Electronics Engineers (IEEE) Annual Meeting of Lasers and Electro-Optics Society LEOS), San Jose, California, November 1991.

Session Chairman, Session on Information Processing, Optical Society of America Annual Meeting, Orlando, San Jose, California, November 1991.

Session Chairman, Session on Pattern Recognition, Optical Society of America Annual Meeting, Orlando, Florida, October 1989.

Session Chairman, Session on Information Processing, Pattern Recognition, and Neural Networks, Institute of Electrical and Electronics Engineers (IEEE) Annual Meeting of Systems, Man, And Cybernetics Society, Cambridge, Massachusetts, November 1989.

Journal Guest Editor: Special Issue of the Journal of Optical Engineering on Optical Information Processing, May 1989.

VIII. Refereed Journal Papers and Books

B. Javidi, Qing Tang, and Don Gregory, " Experiments on Nonlinear Joint Transform Correlators using an Optically Addressed SLM in the Fourier ," *Applied Optics*, Vol. 30, No. 14, pp. 1772-1776, May 10, 1991.

B. Javidi et. al., " Performance of the Binary Joint Transform Correlator in the Presence of the Fourier Plane Quantization," *Journal of Optics Communications*, Vol. 80, pp. 275-284, January 1, 1991.

B. Javidi et. al., " Nonlinearly Transformed Baseband Matched Filters for Optical Pattern Recognition," *Applied Optics*, Vol. 30, No. 14, pp. 1776-1780, May 10 , 1991.

B. Javidi and Jun Wang, " Binary Nonlinear Joint Transform Correlation with Median and Subset Median Thresholding," *Applied Optics*, Vol. 30, No. 8, pp. 967-976, March 10, 1991.

B. Javidi and Qing Tang, " Binary Encoding of Gray Scale Nonlinear Joint Transform Correlators," *Applied Optics*, Vol. 30, No. 11, pp. 1321-1325, April 10, 1991.

B. Javidi et. al., "Quantization and Truncation Effects on Binary Joint Transform Correlation," *Journal of Optics Communications*, Vol. 84, pp. 374-382, August 1, 1991.

B. Javidi, "Generalization of the Linear Matched Filter Concept to Nonlinear Matched Filters," *Applied Optics*, Vol. 29, No. 8, March 10, 1990.

B. Javidi, "Comparison of Nonlinear Joint Transform Image Correlators and Nonlinearly Transformed Matched Filter Based Correlators," *Optical Engineering*, Vol. 29, No. 9, September 1990.

B. Javidi et. al., "Image Enhancement by Nonlinear Signal Processing," *Applied Optics*, Vol. 29, No. 32, November 10, 1990.

B. Javidi et. al., "Image Deconvolution with a Log/Exponential Nonlinear Joint Transform Correlator," *Applied Optics*, Vol. 29, No. 5, February 10, 1990.

B. Javidi, "Nonlinear Joint Power Spectrum Based Optical Correlation," *Applied Optics*, Vol. 28, No. 12, June 15, 1989.

B. Javidi and J. L. Horner, "Multifunction Nonlinear Optical Processor," *Optical Engineering*, Vol. 28, No. 8, August 1989.

B. Javidi, "Nonlinear Matched Filter Based Optical Pattern recognition," *Applied Optics*, Vol. 28, No. 21, November 1, 1989.

Books Edited:

B. Javidi, ed., Optical Information Processing Systems and Architectures I, II, and III, Optical Engineering (SPIE) Publications, 1989, 1990, and 1991.

IX. Invited Papers in Conferences:

B. Javidi, " Optical Pattern Recognition with Nonlinear Techniques in the Fourier Domain", Critical Review of Optical Pattern Recognition, OPTCON 91 (Sponsored by IEEE Lasers Electro-Optics Society, Optical Society of America, and the Optical Engineering Society) , San Jose, California, November 3-8, 1991.

B. Javidi, " Grey Scale Optical Image Processing with Binary Encoding Techniques in the Fourier Domain", the Annual Meeting of the IEEE Lasers Electro-Optics Society, OPTCON 91 (Sponsored by IEEE Lasers Electro-Optics Society, Optical Society of America, and the Optical Engineering Society) , San Jose, California, November 3-8, 1991.

B. Javidi, " Optical Attentive Associative Memory with Channel Dependent Nonlinearities in the Weight Plane", Proceedings of the IEEE International Conference on Systems, Man, and Cybernetics Society, Vol II, pp. 415-420, November 1989.

X.Honors:

1990 National Science Foundation Presidential Young Investigator

XI. Milestones:

1. Generalization of the linear matched filter concept to nonlinearly transformed matched filters

2. Image deconvolution using a nonlinear joint transform processor
3. Image Enhancement by Nonlinear Signal Processing
4. Optical implementation of nonlinear joint transform correlators using both optically addressed spatial light modulators (SLMs) and electrically addressed SLMs
5. Quantization and truncation effects on binary joint transform correlation

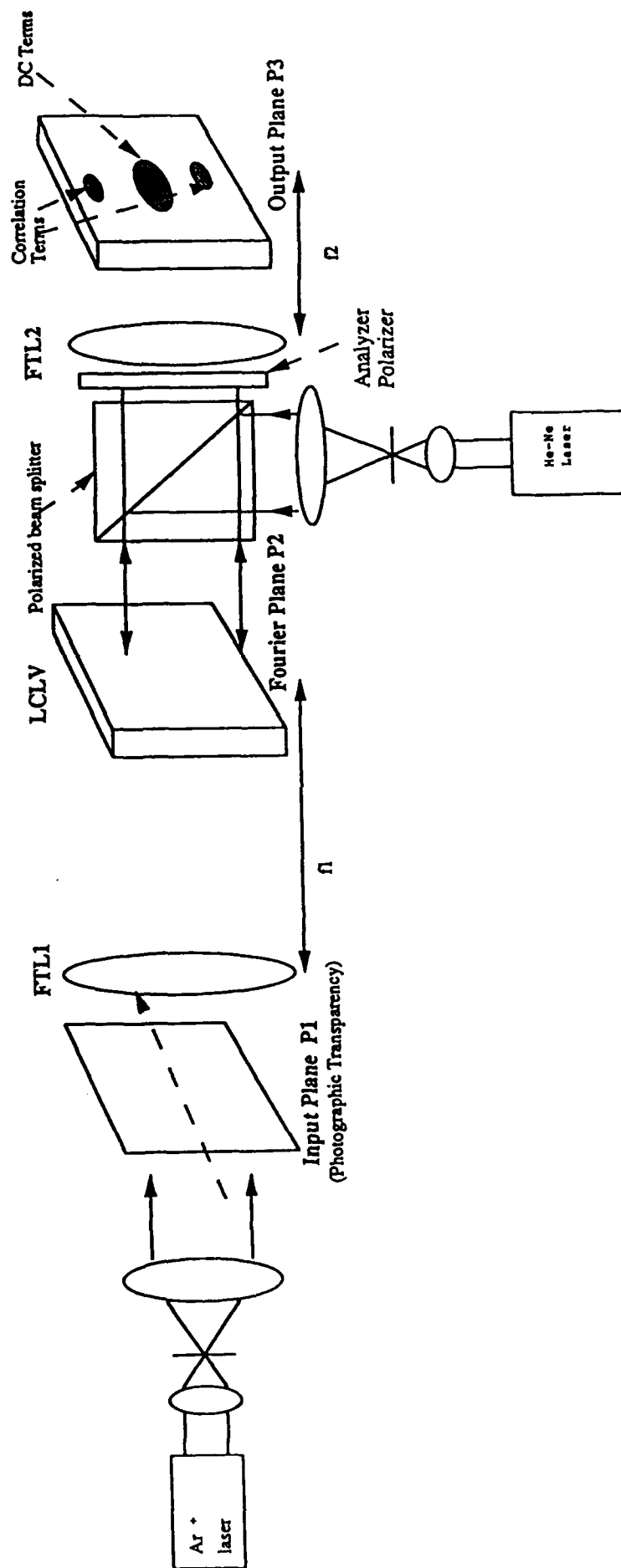


Figure 1. Nonlinear joint transform correlator using a liquid crystal light valve (LCLV) at the Fourier plane



Figure 2. Image used in the correlation tests. The tank is the reference image.

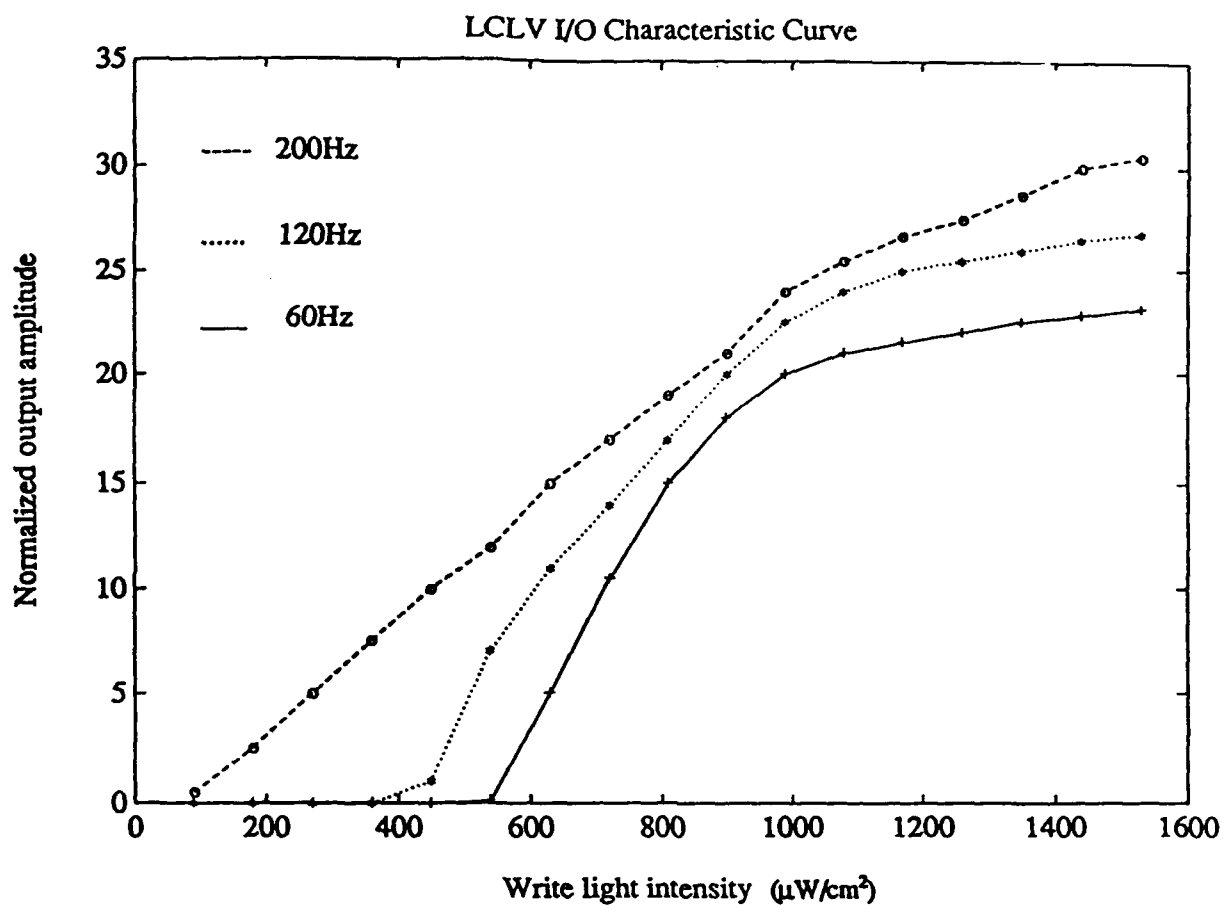


Figure 3. Input-output characteristic curves of the LCLV for three different power supply frequencies applied to the LCLV. The bias supply voltage is 10Vrms.

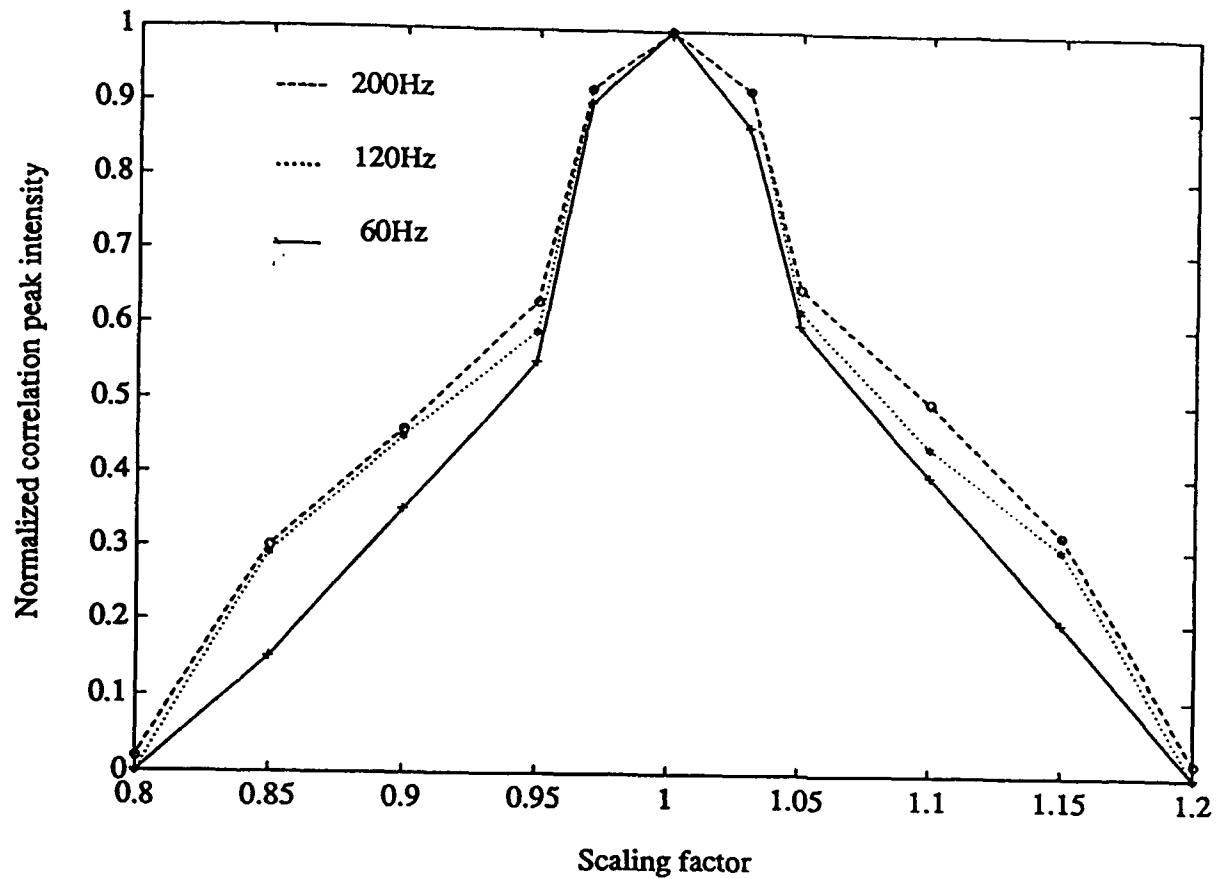


Figure 4(a). Variations in the normalized correlation peak intensity versus the scale factor of the input signal for correlation of the tank and the tank. Triangles correspond to the 200Hz curve, circles correspond to the 120 Hz curve, and crosses correspond to the 60Hz curve.

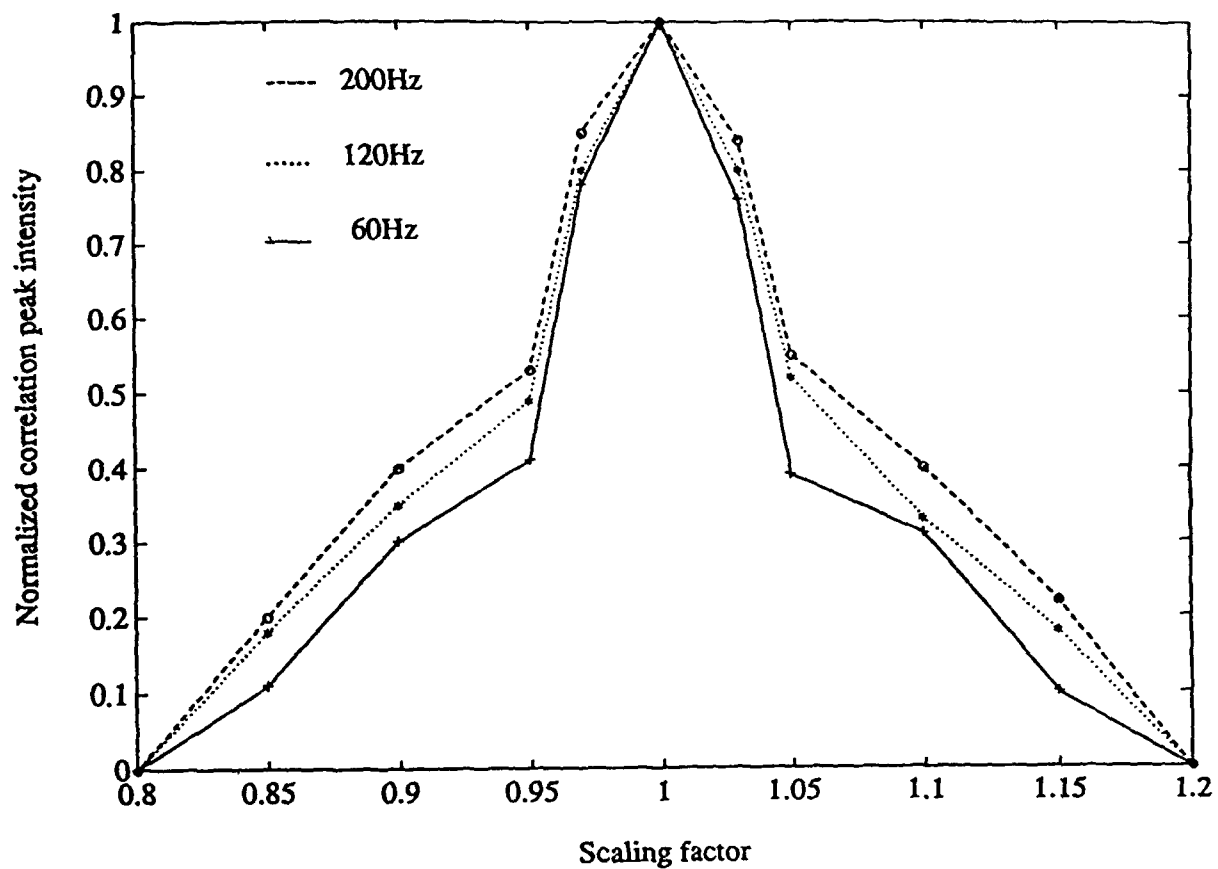


Figure 4(b). The same as Fig. 4(a), except for correlation of the tank and the tank in the input scene noise.

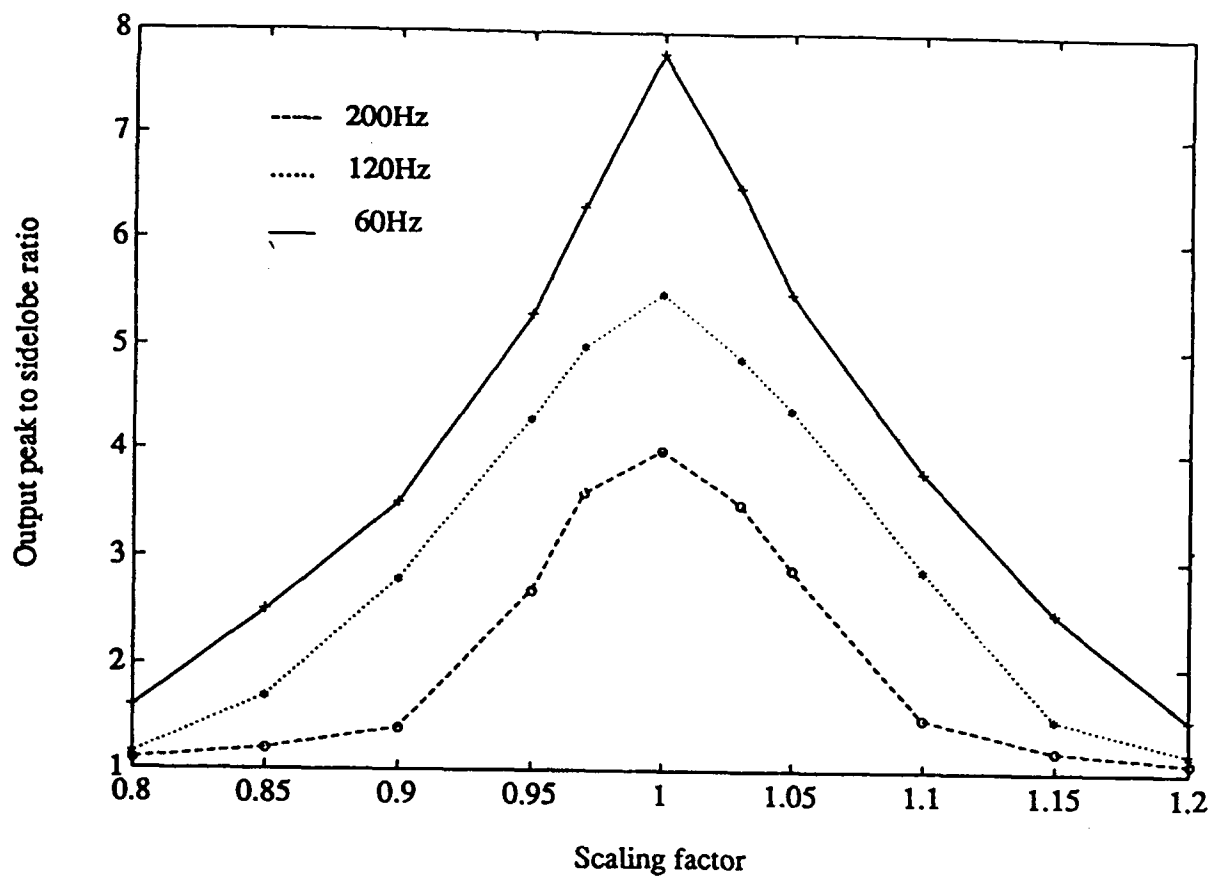


Figure 5(a). Variations in the correlation peak to sidelobe ratio versus the scale factor of the input signal for correlation of the tank and the tank. Triangles correspond to the 200Hz curve, circles correspond to the 120 Hz curve, and crosses correspond to the 60Hz curve.

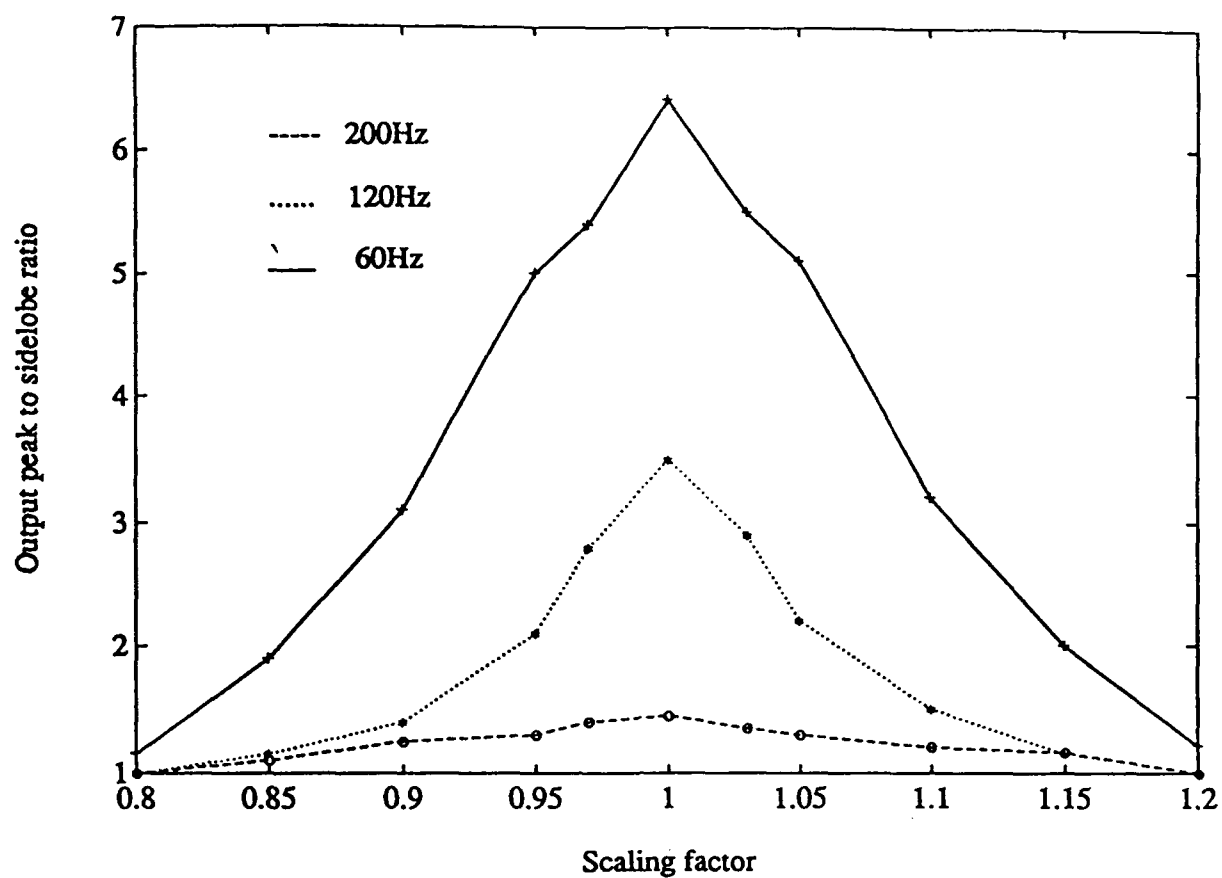


Figure 5(b). The same as Fig. 5(a), except for correlation of the tank and the tank in the input scene noise.

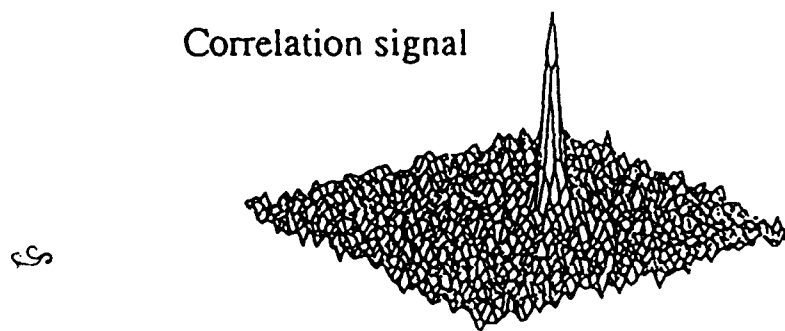
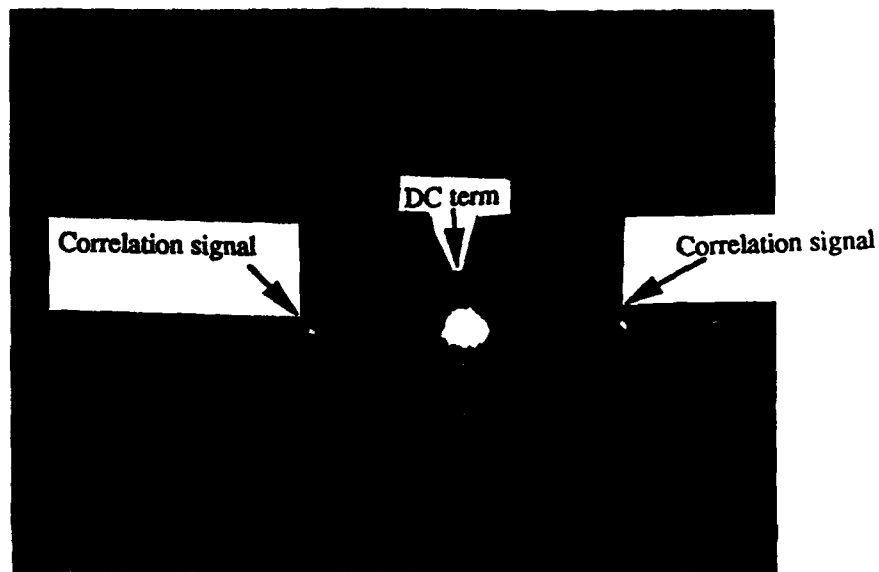


Figure 6(a). Photograph of the nonlinear JTC output of the tank and the tank in the input scene noise for no rotational or scale changes of the input image. The liquid crystal light valve is operating along the 200Hz curve. The 3-D plots of the correlation signals are also shown. The 3-D plots are normalized to a maximum value of unity. The DC terms are not shown in the 3-D plots.

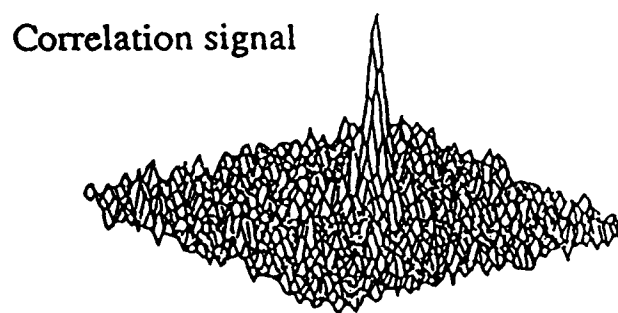
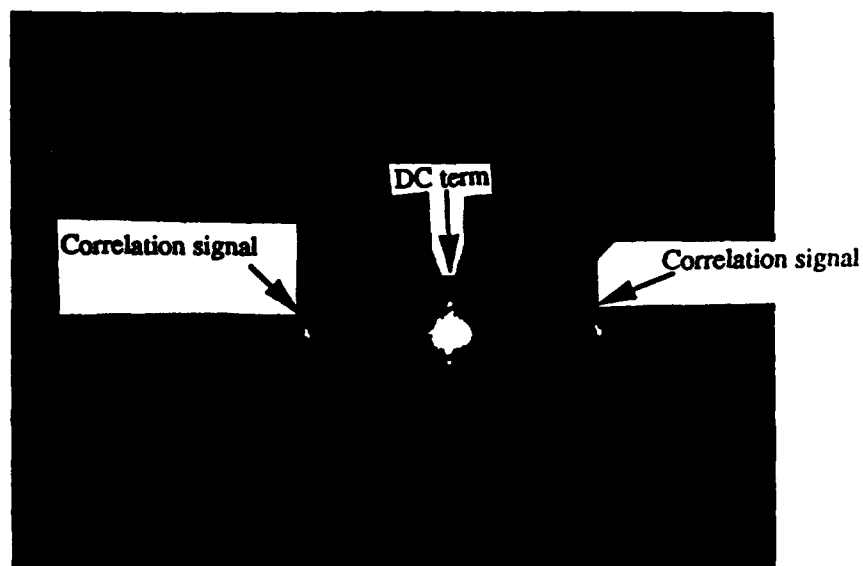


Figure 6(b). The same as Fig. 6(a), except that the liquid crystal light valve is operating along the 60Hz curve.

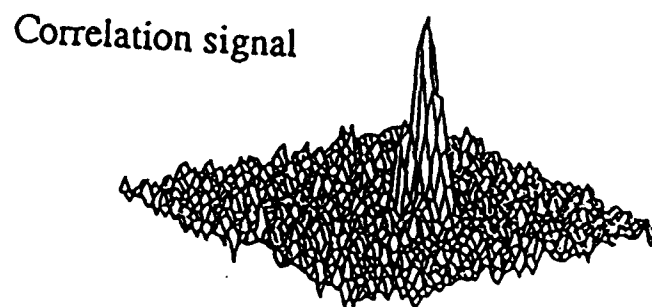
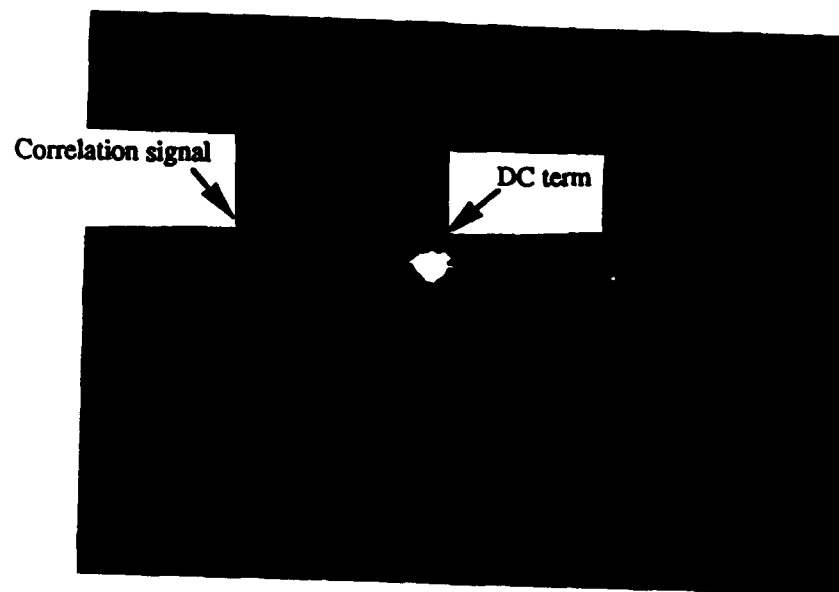


Figure 7(a). Photograph of the nonlinear JTC output of the tank and the tank in the input scene noise for a scaling change of 1.05. The liquid crystal light valve is operating along the 200Hz curve. The 3-D plots of the correlation signals are also shown. The 3-D plots are normalized to a maximum value of unity. The DC terms are not shown in the 3-D plots.

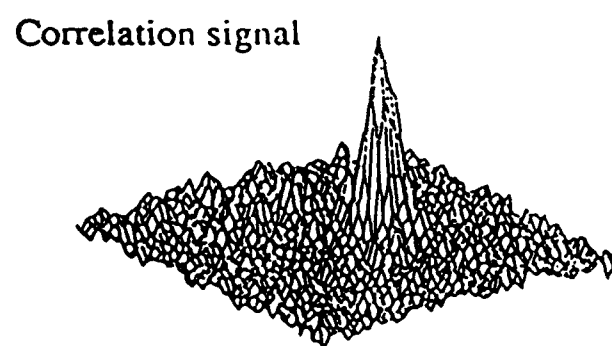
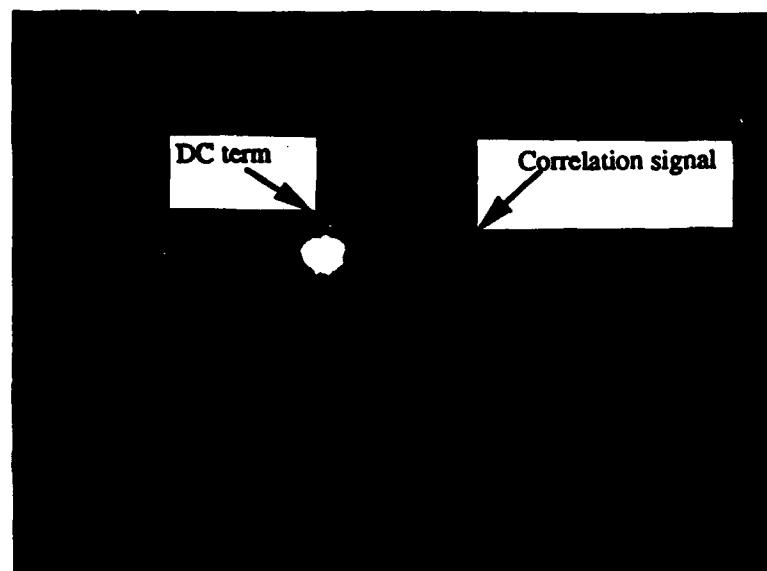


Figure 7(b). The same as Fig. 7(a), except that the liquid crystal light valve is operating along the 60Hz curve.

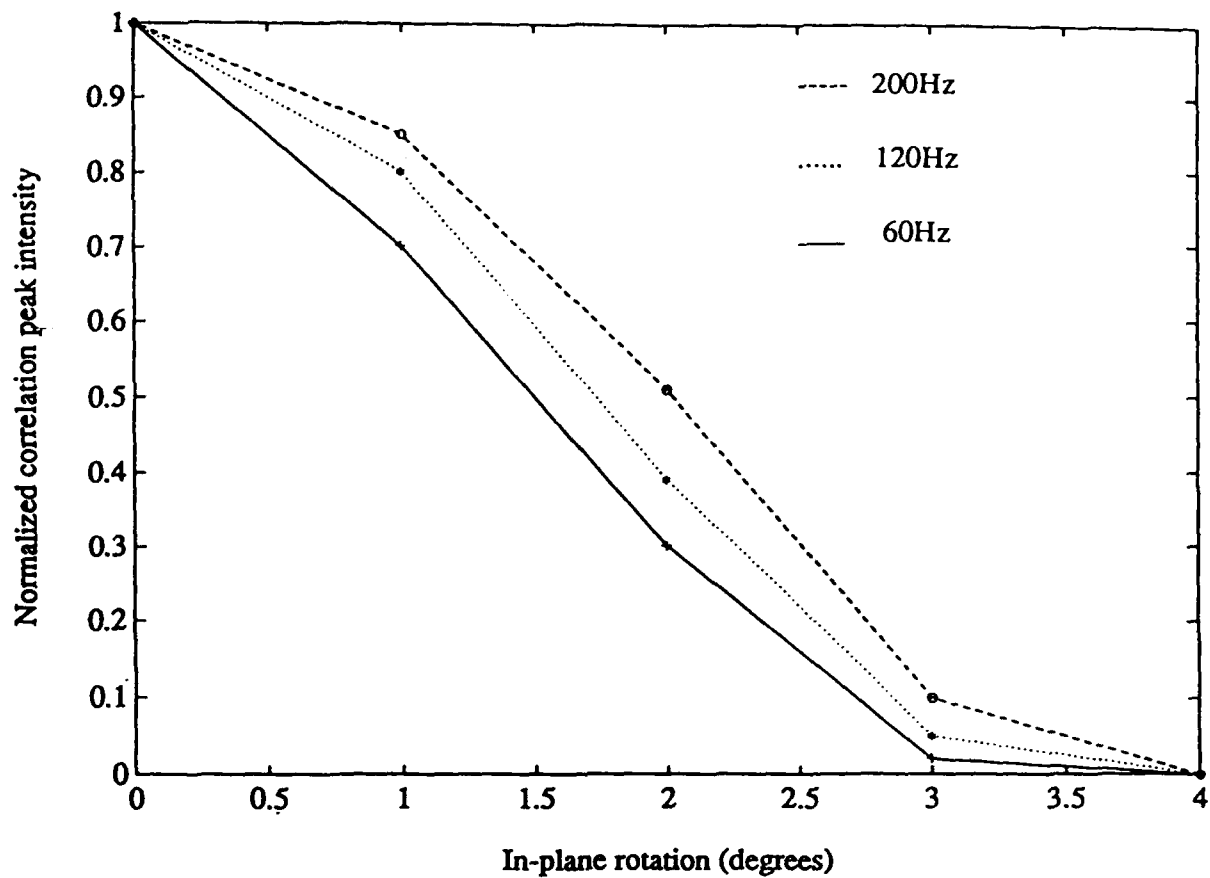


Figure 8(a). Variations in the normalized correlation peak intensity versus the rotation factor of the input signal for correlation of the tank and the tank. Triangles correspond to the 200Hz curve, circles correspond to the 120 Hz curve, and crosses correspond to the 60Hz curve.

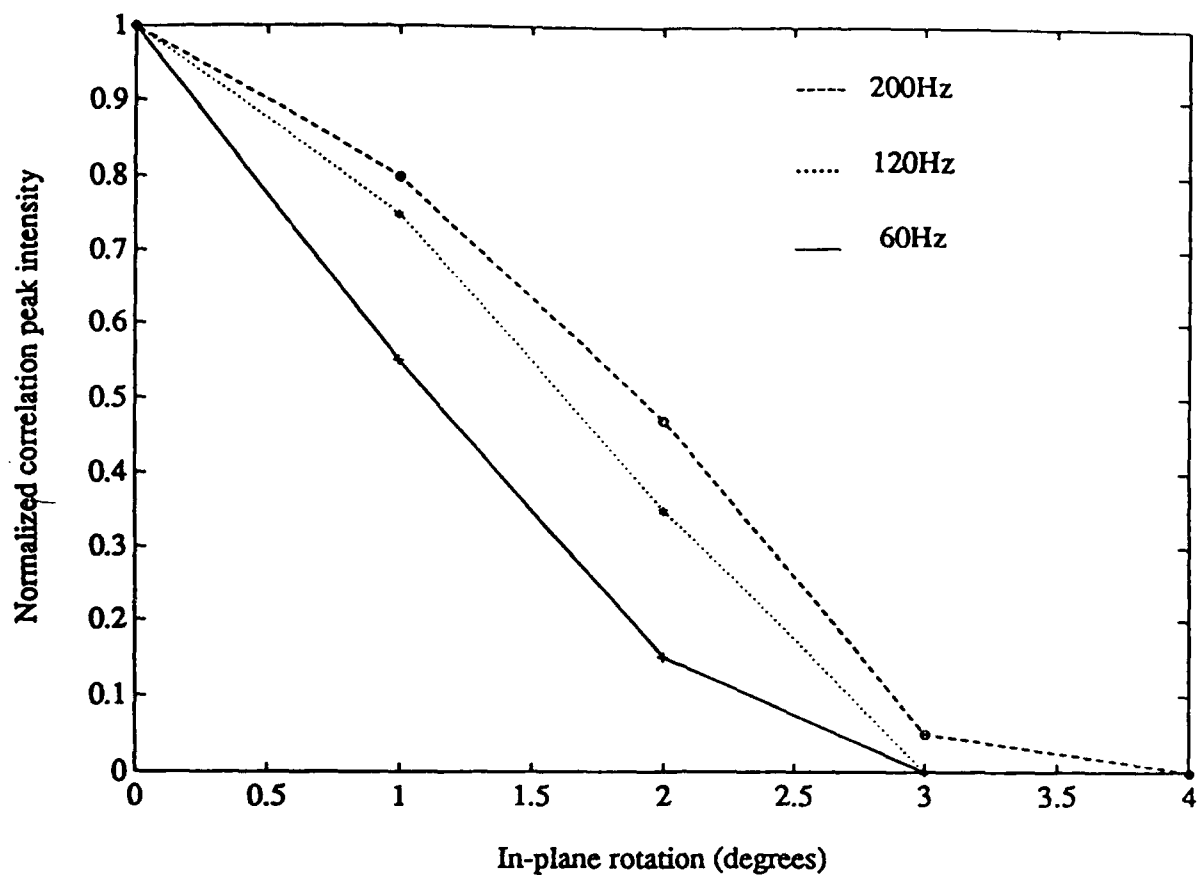


Figure 8(b). The same as Fig. 8(a), except for correlation of the tank and the tank in the input scene noise.

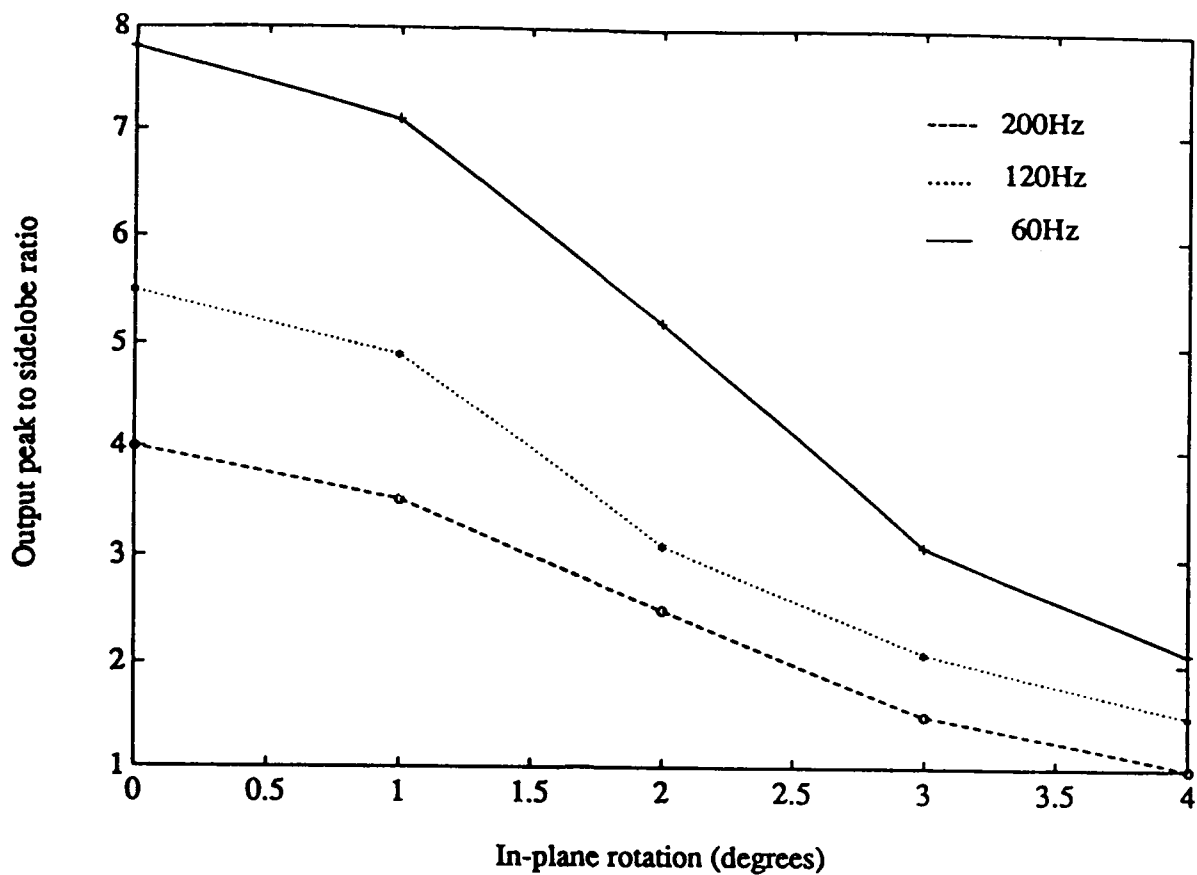


Figure 9(a). Variations in the correlation peak to sidelobe ratio versus the rotation factor of the input signal for correlation of the tank and the tank. Triangles correspond to the 200Hz curve, circles correspond to the 120 Hz curve, and crosses correspond to the 60Hz curve.

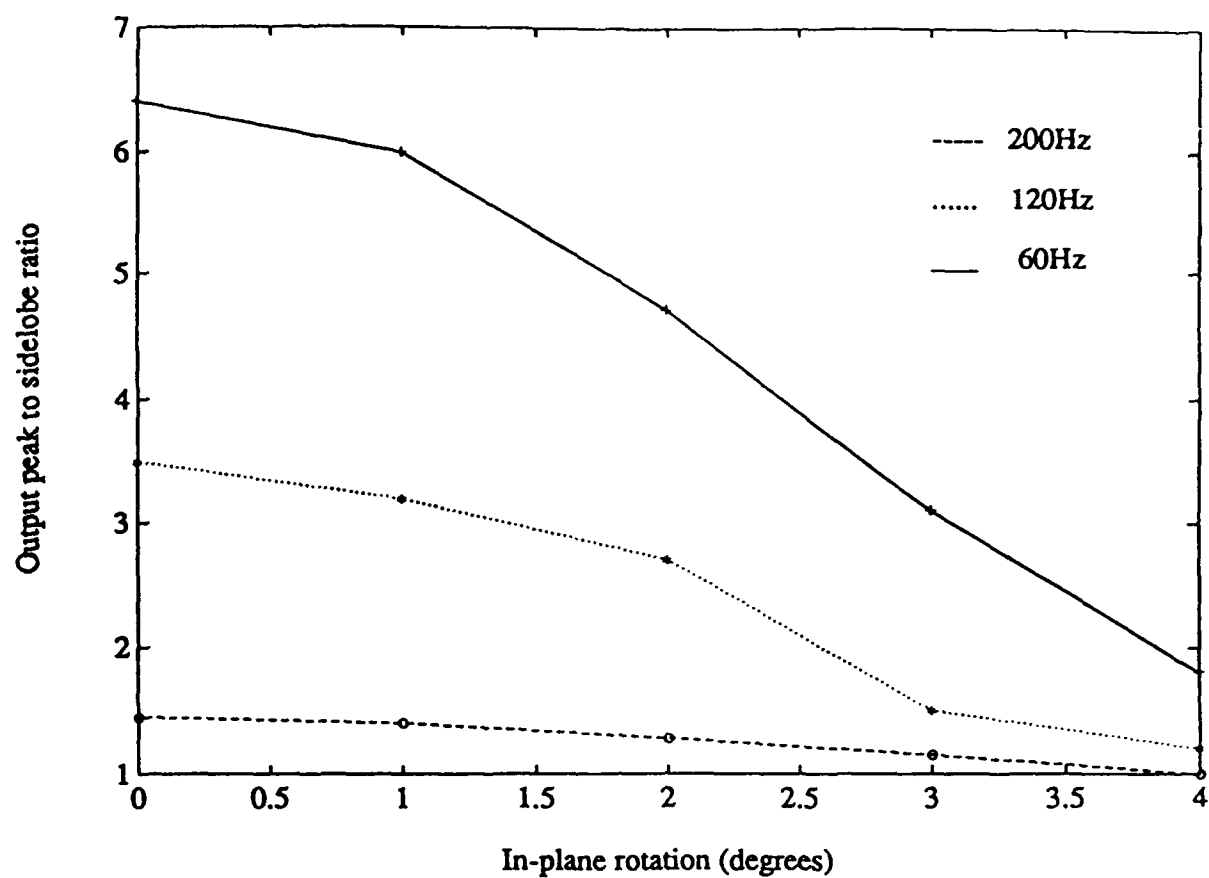


Figure 9(b). The same as Fig. 9(a), except for correlation of the tank and the tank in the input scene noise.

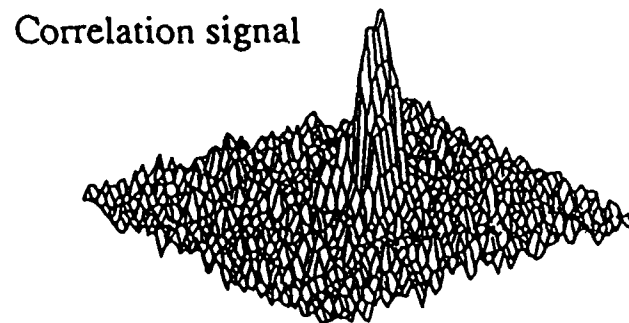
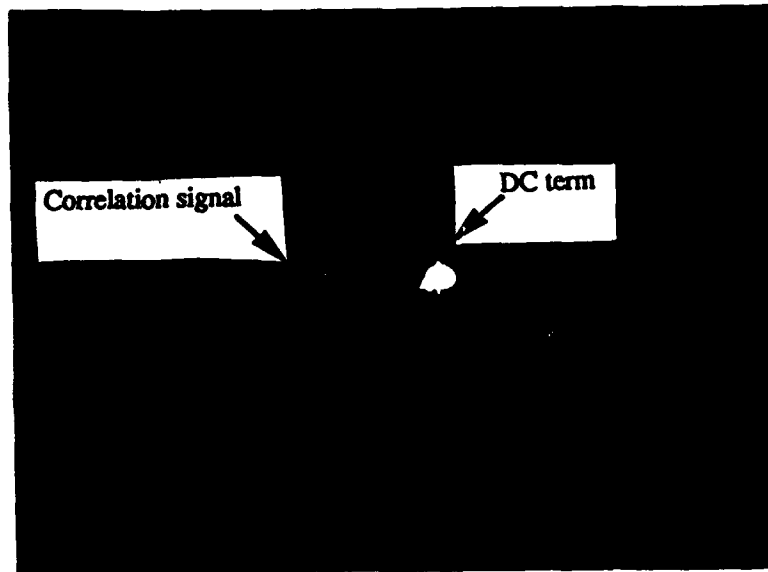
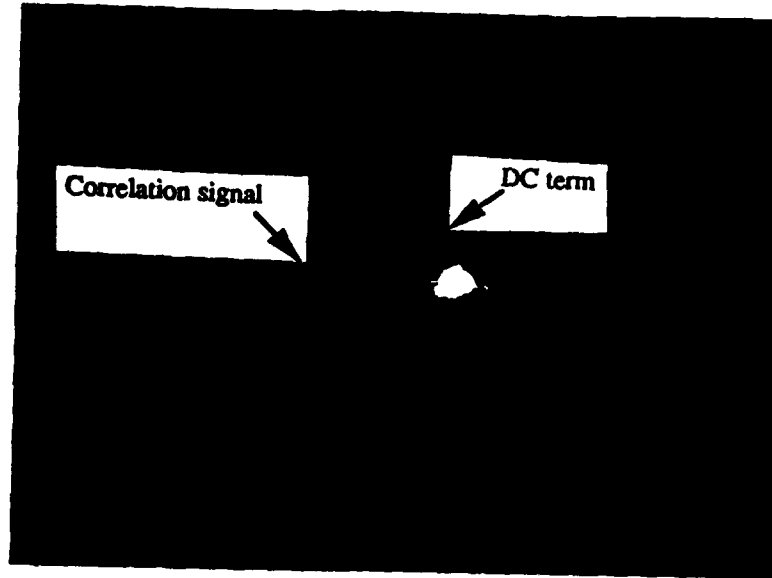


Figure 10(a). Photograph of the nonlinear JTC output of the tank and the tank in the input scene noise for a rotational change of 2 degrees. The liquid crystal light valve (LCLV) is operating along the 200Hz curve. The 3-D plots of the correlation signals are also shown. The 3-D plots are normalized to a maximum value of unity. The DC terms are not shown in the 3-D plots.



Correlation signal

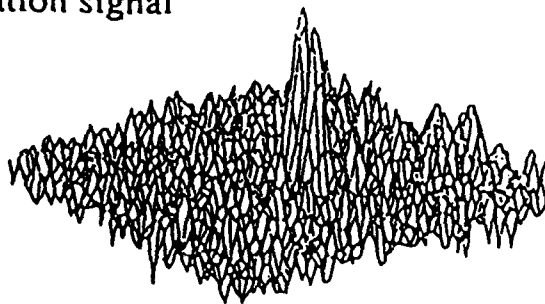


Figure 10(b). The same as Fig. 10(a), except that the liquid crystal light valve (LCLV) is operating along the 60Hz curve.

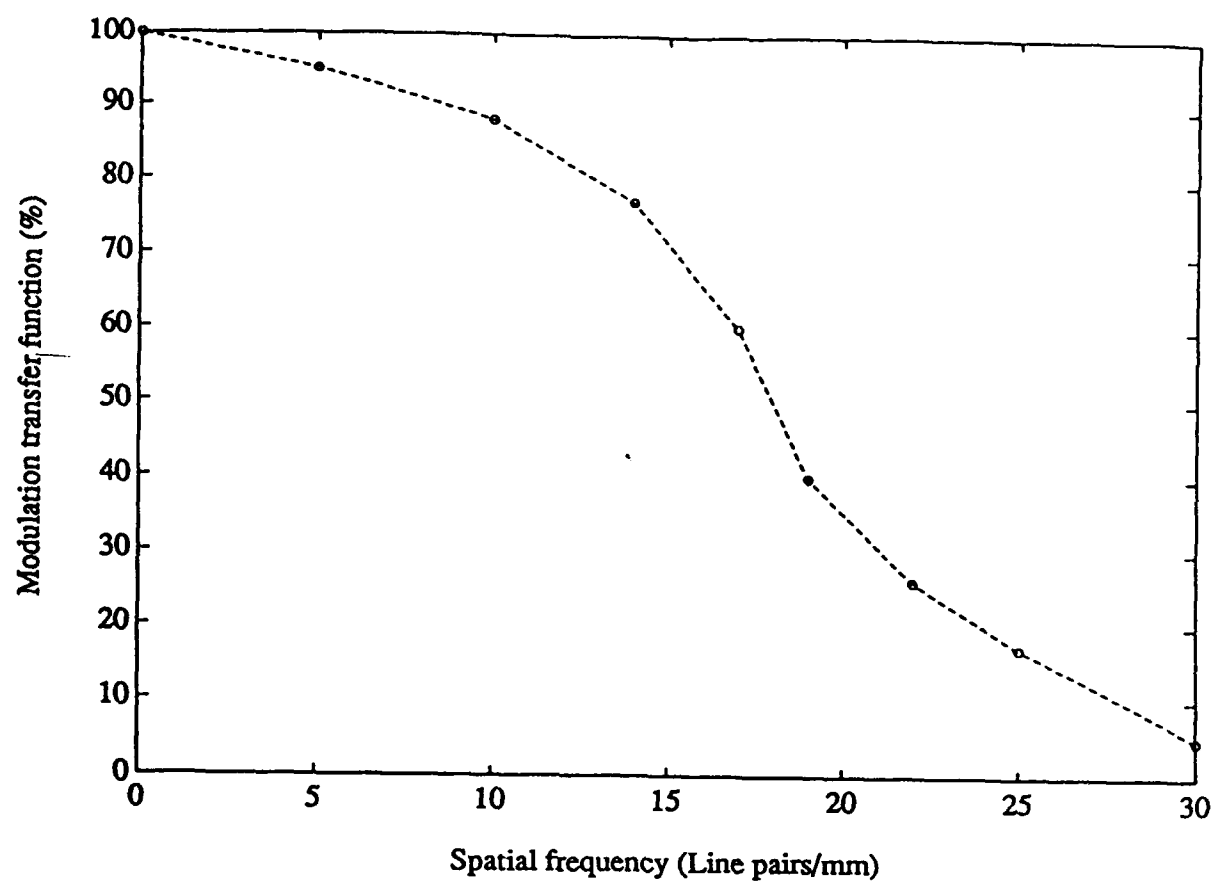


Figure 11. Modulation Transfer Function (MTF) of the liquid crystal light valve (LCLV) used in the experiments.

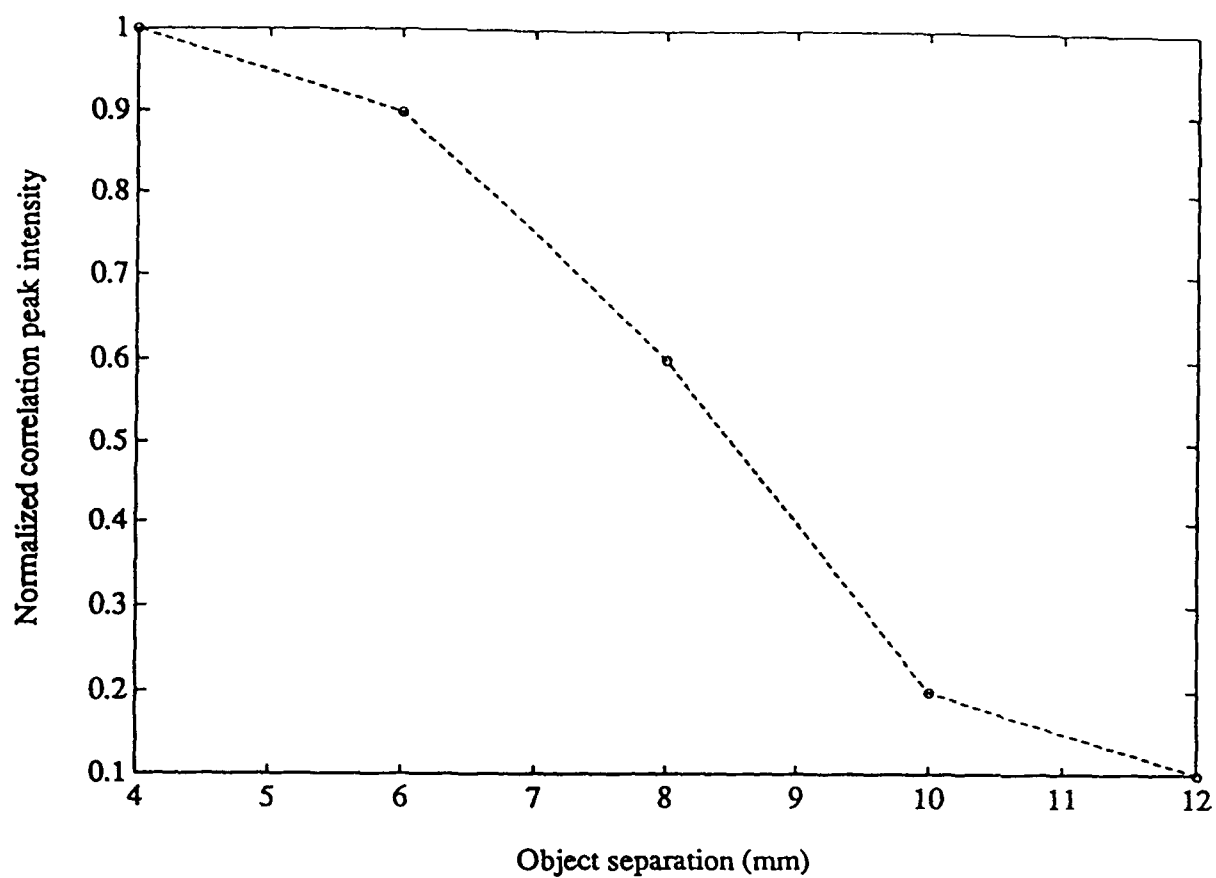


Figure 12. Normalized correlation peak intensity versus the separation of the input objects.

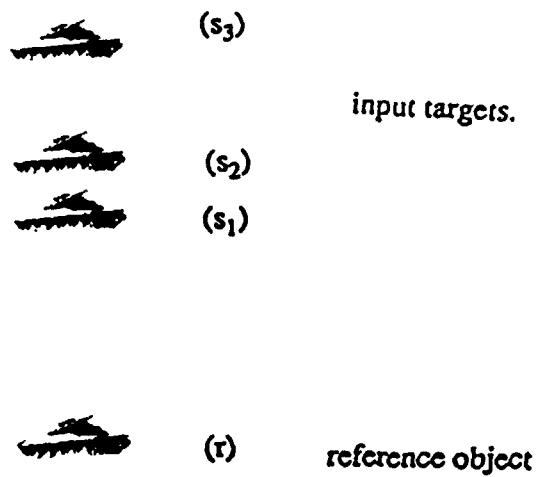


Figure 13. The reference object and the input targets for a multiobject nonlinear JTC experiment. The reference object is denoted by r , and the input targets are denoted by s_1 , s_2 , and s_3 .

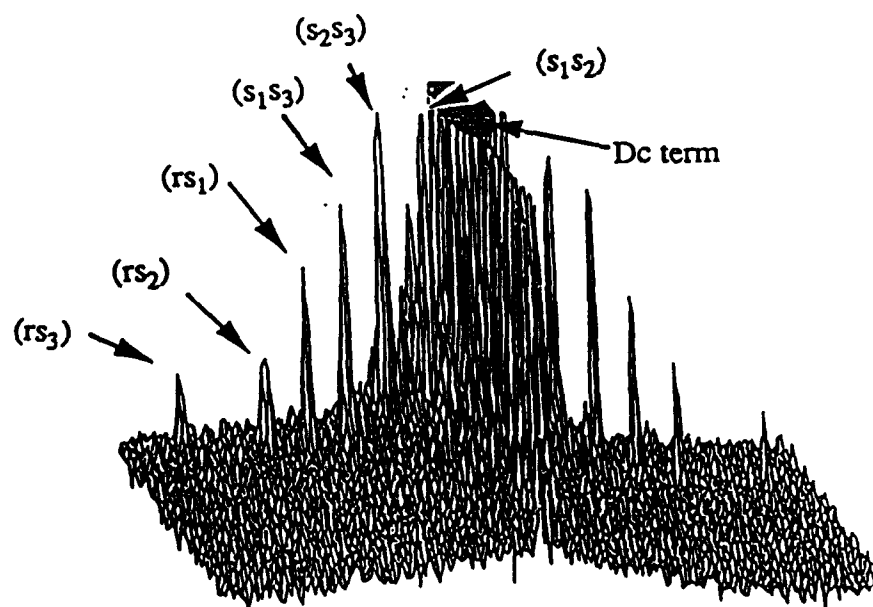
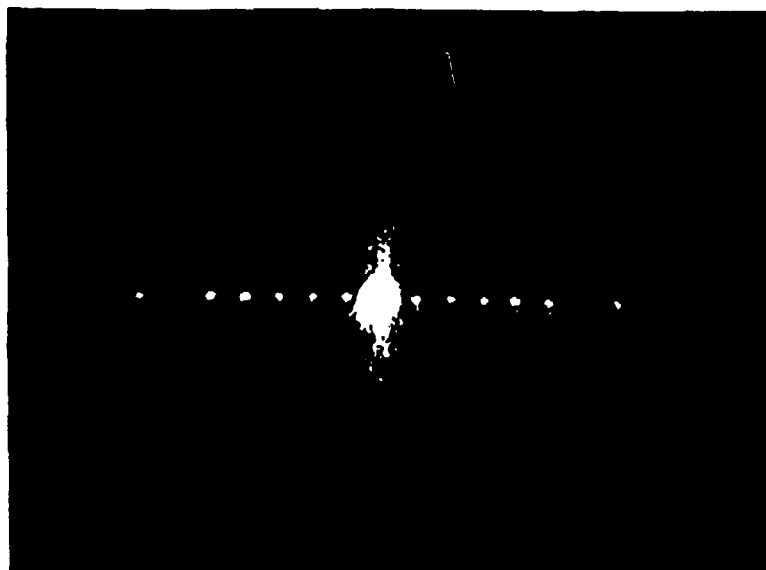


Figure 14. Photograph of the nonlinear JTC output of the tank and the input scene with three tanks [see Fig. (13)]. The 3-D plot of nonlinear JTC output is also shown. The correlations between the reference object and the input targets are denoted by rs_i , and the correlations between the input targets are denoted by $s_i s_j$

**MISSION
OF
ROME LABORATORY**

Rome Laboratory plans and executes an interdisciplinary program in research, development, test, and technology transition in support of Air Force Command, Control, Communications and Intelligence (C³I) activities for all Air Force platforms. It also executes selected acquisition programs in several areas of expertise. Technical and engineering support within areas of competence is provided to ESD Program Offices (POs) and other ESD elements to perform effective acquisition of C³I systems. In addition, Rome Laboratory's technology supports other AFSC Product Divisions, the Air Force user community, and other DOD and non-DOD agencies. Rome Laboratory maintains technical competence and research programs in areas including, but not limited to, communications, command and control, battle management, intelligence information processing, computational sciences and software producibility, wide area surveillance/sensors, signal processing, solid state sciences, photonics, electromagnetic technology, superconductivity, and electronic reliability/maintainability and testability.